PHYSICAL REVIEW B **76**, 041402(R) (2007)

Wetting transition of water on graphite: Monte Carlo simulations

Xiongce Zhao*
Center for Nanophase Materials Sciences, Oak Ridge National Laboratory, Oak Ridge, Tennessee 37831, USA
(Received 23 February 2007; revised manuscript received 24 May 2007; published 19 July 2007)

We report evidence observed from molecular simulations for the first-order wetting transition of water on a solid surface. Based on the empirical potentials of SPC/E for water, the 10-4-3 van der Waals model, and a recently developed induction and multipolar potential for water and graphite, we show through a series of Monte Carlo simulations that the first-order wetting transition of water on graphite occurs at 475–480 K, and the prewetting critical temperature lies in the range 505–510 K. The calculated wetting transition temperature agrees quantitatively with that predicted previously using a simple model.

DOI: 10.1103/PhysRevB.76.041402 PACS number(s): 68.35.Rh, 64.70.Fx, 82.20.Wt

When a fluid adsorbs on a solid surface at temperatures below the fluid critical temperature (T_c), the adsorbed film either spreads across the surface (wetting) or beads up as a droplet (nonwetting) as the pressure approaches the saturated vapor pressure P_{svp} of the fluid. The wetting transition describes the transition between those two kinds of behavior. An analysis of wetting transition was first presented 30 years ago by Cahn[1] and Ebner and Saam[2] (CES). They showed that if a fluid does not wet a particular surface at low temperature, then the system ought to exhibit wetting transition at some temperature T_w below the critical point T_c. In terms of adsorption isotherms, the wetting phenomenon should manifest itself as following three different patterns. (1) At temperatures below T_w, adsorption beginning with a thin film increases slightly as the pressure increases toward P_{svp}. At P_{svp} the bulk vapor condenses, and the adsorption coverage abruptly becomes infinite. On a coverage vs pressure diagram, the adsorption isotherm reaches P_{svp} with a discontinuous jump (infinite slope). (2) In the temperature range between T_w and the prewetting critical temperature T_{pwc}, the thin film grows as the pressure increases until it jumps to a thick, liquidlike film of finite thickness at some pressure less than P_{svp}. This thin-to-finite film or wetting transition is followed by continuous growth until condensation occurs at P_{svp}. (3) At temperatures higher than T_{pwc}, the film grows continuously and the prewetting transition disappears.

Since work of CES, a variety of experimental[3–16] and theoretical studies[17–30] have been performed on the wetting transition of fluids on various solid surfaces. Finn and Monson[18] were among the first to calculate the wetting temperature of fluid on solid surface by using Monte Carlo (MC) simulation methods. They predicted the wetting behavior of Ar on solid CO_2 surface using isobaric-isothermal MC simulations. This system was re-evaluated by Shi *et al.*[31] and Errington[30] using different simulation approaches. Other simulation studies were primarily focused on simple atomistic fluids such as inert gases or H_2 isotopes on alkali metal surfaces.[25,26,28]

No wetting transition has ever been observed for any molecular fluids on solids other than hydrogen and its isotopes, which are essentially spherical molecules. Being the most important fluid, the adhesive and lubricative properties of water are of immense fundamental interest to a wide range of communities. But to our knowledge, never before has wetting transition been predicted for water on any solid surface using a realistic model and simulation method. It is known that water does not wet many surfaces (such as graphite) at room temperature. Theoretically, the wetting transition of water on graphite is expected to occur at a temperature below its bulk critical temperature. Recently, Gatica *et al.*[29] estimated, using a simple model, that a wetting transition of water on graphite would occur around 474 K. In this Rapid Communication, we report evidence for a first-order wetting transition of water on graphite from molecular simulations. In addition, we calculate T_w and T_{pwc} of water on graphite using Monte Carlo simulations.

The water-water interaction is described by the SPC/E model.[32] This model was chosen because its critical temperature is 635 K, which is the closest to the experimental value (647 K) compared with the predictions by many other popular nonpolarizable water potentials.[33] It is known that the ability of an interaction potential to describe the bulk critical behavior is a necessary (though not sufficient) requirement in order for it to predict the wetting behavior of the fluid on a surface.[34] The graphite surface is modeled as a smooth basal plane. The Lennard-Jones (LJ) interaction between water and graphite is given by the 10-4-3 potential.[35] A recently developed effective potential for polar fluids and graphite[36] is used to describe the polar and induction interactions between water and graphite. Details of the SPC/E, 10-4-3, and polar potentials can be found in the literature.[32,35,36]

We have used grand canonical Monte Carlo (GCMC) simulations combined with the multiple histogram reweighting (MHR) method[37] to compute the saturated coexistence chemical potentials (μ_{svp}) and adsorption isotherms of water on graphite at various temperatures. The MHR provides very precise values of μ_{svp} through the equal area criterion,[38] which is very important for studying wetting transitions. The GCMC cell is a rectangular box with volume of $2000\sigma_f^3$ and height in the z direction of $15\sigma_f$, where σ_f is the LJ diameter of the SPC/E potential. The lower plane normal to the z axis is modeled as the graphite surface and the opposite plane as a hard repulsive wall. The hard wall is always completely dry to the liquid phase at bulk coexistence, which helps to suppress capillary condensation.[39] Special care was taken to choose the height of the cell. We performed trial simulations using different cell heights ranging from $10\sigma_f$ to $50\sigma_f$ at temperatures and pressures of interest. It was found that the adsorption properties obtained at $15\sigma_f$ are consistent with

those obtained at $20\sigma_f$, $30\sigma_f$, $40\sigma_f$, and $50\sigma_f$ within the statistical fluctuations. This indicates that $15\sigma_f$ is adequate for simulating the adorption and prewetting behavior of the system. Two-dimensional periodic boundary conditions were applied in the lateral x and y directions. Each simulation included 80×10^6 and 20×10^6 MC moves for equilibration and production, respectively, with histograms collected every 20 MC moves during the production. The LJ cutoff was 0.9 nm without long-range correction. Ewald summations were used to calculate the electrostatics. A pseudo-two-dimensional Ewald summation method[40] was used in adsorption simulations.

Based on the predicted T_w reported in Gatica *et al.*'s work, we chose to perform GCMC simulations at 460, 470, 480, 490, 500, and 510 K with varying reduced chemical potentials to obtain the histograms for the bulk water and water/graphite adsorption systems. We used the method proposed by Shi *et al.*[31] to check the overlap of histograms for any two adjacent state points. Preliminary simulations indicated that T_w lies between 470 to 480 K and T_{pwc} between 500 and 510 K. Therefore, additional simulations at 475 and 505 K were performed to narrow down T_w and T_{pwc}.

For convenience of presentation, we define the parameter χ^* as

$$\chi^* = \exp\left(\frac{\mu^* - \mu^*_{svp}}{T^*}\right),$$

where μ^* is the reduced chemical potential of bulk water and μ^*_{svp} is the saturation chemical potential of bulk water at the reduced temperature T^*. Plotting the adsorption coverage versus χ^* enables one to identify the transition feature without ambiguity. The parameter χ^* is the ratio of the activity to the activity at saturation, with $\chi^*=1$ corresponding to $\mu^*=\mu^*_{svp}$ or $P=P_{svp}$. Additionally, $\chi^*=P/P_{svp}$ if ideal behavior is assumed in the bulk vapor phase. However, water vapor cannot be treated as an ideal gas under temperatures interested in this study.

GCMC simulations were carried out for μ^* up to saturation under each temperature. As μ^* was increased toward μ^*_{svp}, three different types of behavior in the growth of the adsorption film were observed, corresponding to three ranges of temperature. Adsorption isotherms for water/graphite at several representative temperatures are shown in Fig. 1.

At temperatures below 475 K, the adsorption coverage is minuscule until μ^*_{svp} is reached, which indicates partial wetting or nonwetting. The isotherm jumps to the saturated liquid density at χ^*_{svp}, which can be seen from Fig. 1 and the density profile growth patterns shown in Fig. 2(a). The sharp increase of density between $\chi^*=0.991$ and 1.008 corresponds to a first-order transition from nonwetting to liquid condensation. At $\chi^*=1.008$, much of the density profile becomes comparable with the saturated liquid density profile (the saturated liquid density at 475 K is $\rho^*\approx0.89$ from bulk simulations), except the first peak corresponds to the density of liquid film in contact with the wall.

In contrast, the simulation results at temperatures between 480 and 505 K manifest quite different behavior. Initially the coverage forms a thin film. As μ^* increases, the thin film

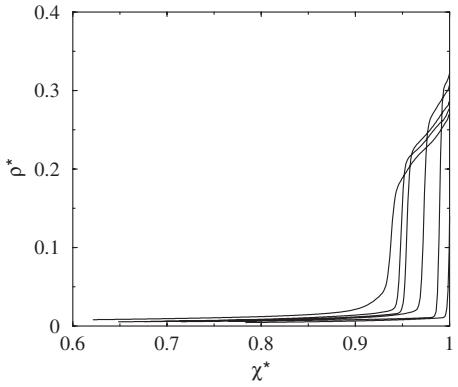

FIG. 1. Adsorption isotherms of water on graphite from GCMC simulations and MHR, where ρ^* is the reduced number density. The curves correspond to $T=510$, 505, 500, 490, 480, and 475 K, from left to right.

thickens abruptly to a finite thickness, which indicates a wetting behavior (Fig. 1). The wetting transition is followed by continuous growth until condensation occurs at μ^*_{svp}. The transition feature is more clearly shown by the density profile growth in Fig. 2. Taking the isotherm at 490 K as an example, there is sudden jump in adsorption from minimum to a finite coverage at $\chi^*=0.965$ to 0.972 [Fig. 2(b)]. But apparently the increased coverage does not correspond to a liquid condensation (saturated liquid density at 490 K is $\rho^*\approx0.85$). Afterward, the film grows continuously until condensation occurs at μ^*_{svp}. Thus, the results shown in Figs. 1 and 2(b) are clear evidence for the wetting transition of water on graphite, with a wetting temperature somewhere between 475 and 480 K, i.e., $T_w=475-480$ K.

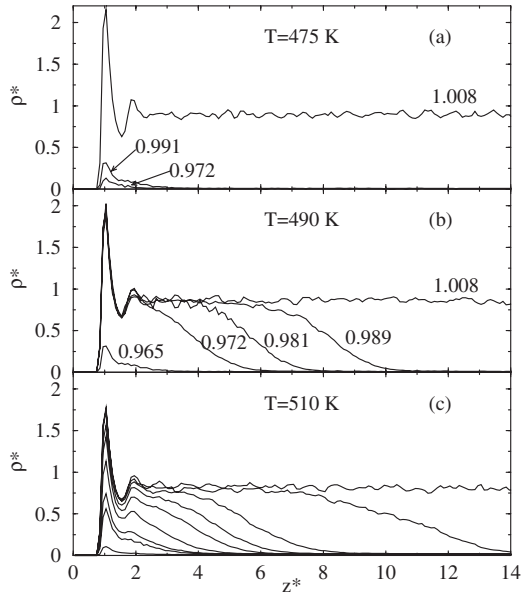

FIG. 2. Local density profiles for water adsorption on graphite as a function of reduced distance from the surface, $z^*=z/\sigma_f$. $T=$(a) 475, (b) 490, and (c) 510 K. In (a) and (b), the values of χ^* at which the calculations were performed are indicated by the labels in the graph. In (c), profile curves are for $\chi^*=$ 0.731, 0.878, 0.892, 0.919, 0.940, 0.962, 0.977, 0.995, and 1.003, from bottom to top.

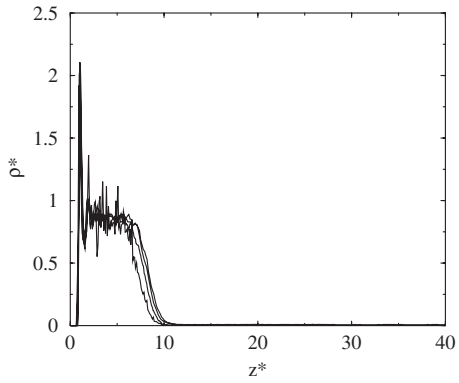

FIG. 3. Film density for water on graphite at $T=490$ K and $\chi^*=0.992$. Curves correspond to varying heights of the simulation cell, $H^*=10$, 20, 40, and 30, from left to right.

At $T=510$ K, the adsorption isotherm becomes continuous as μ^* increases (Fig. 1), which indicates $T_{pwc} \leq 510$ K. As shown by the growth of density profiles in Fig. 2(c), the adsorption film builds from a thin to a thick one continuously as μ^* increases to μ^*_{svp}. The density of the first peak in the profiles grows gradually to that of an adsorbed liquid. At μ^*_{svp}, the density profile evolves to the one corresponding to the liquid density except for the first peak adjacent to the wall. The simulation results obtained at 505 and 510 K (Fig. 1) indicate that T_{pwc} of water on graphite lies somewhere between these two temperatures, i.e., $T_{pwc}=505-510$ K.

The nature of the prewetting jump of water on graphite at temperatures 480–505 K can be further shown by the results obtained from simulations at 490 K, $\chi^*=0.992$, with varying simulation dimensions in the surface normal direction. Shown in Fig. 3 are the density profiles obtained from simulations with box height $H^*=h/\sigma_f=10,20,30,40$, respectively. In order to compare the results with consistency, in those four simulations the area of the graphite wall is kept at $10\sigma_f \times 10\sigma_f$. It can be seen from Fig. 3 that the rapid rise of the film thickness to a finite value is independent of H^*. The film thickness remains about $7.5\sigma_f$ under various values of H^*. This is a clear indication that the transition is prewetting rather than capillary condensation, since the only other transition in the system would involve the interface jumping to the very center of the simulation cell for $T>T_w$ at bulk coexistence.

We did not attempt to calculate the exact T_w or T_{pwc} values based on current simulations. There are several factors that might be considered in future studies to improve the accuracy of the simulated results. One of the primary concerns is the realism of the water potential employed. It is known that T_w calculated from simulations depends sensitively on the solid-fluid interaction, as demonstrated by several groups in previous work.[26,28] For example, Shi *et al.* found that a ~10% increase in the surface-fluid attraction decreases the wetting transition temperature of Ar on a CO_2 surface from 25.5 to 22.5 K.[28] In this work, the solid-fluid potential is calculated using the Lorentz-Berthelot mixing rules. The choice of the water potential will affect the graphite-water interaction implicitly, and thus the calculated T_w. The SPC/E water potential gives by far the best predictions for the critical properties of bulk water among all the available nonpolarizable water models, while it still cannot simulate exactly the coexistence properties of bulk water. The accuracy of the estimated T_w and T_{pwc} may be improved by using more accurate polarizable models such as the Gaussian charge polarizable model.[41] In addition, by modeling the graphite as a smooth surface, we neglected the possible impact from surface corrugations and dynamics of the surface structure during the adsorption. A previous simulation work indicates that the impact of surface corrugation of the adsorbent on the transition behavior of Ne is minimal.[25] But it is unclear if the same conclusion is applicable to the graphite-water system.

The wetting transition of water on graphite calculated in this work agrees quantitatively with the previous prediction by Gatica *et al.*[29] using the so-called CCST model,[19] although different water potentials are employed in these two studies. It has been pointed out by Shi *et al.*[28] that the wetting behavior predicted theoretically depends on both the well depth and the shape of the solid-fluid potential. In Gatica *et al.*'s work, the TIP4P potential was used instead of SPC/E for water. We note that the well depth (D) and well width w, which is defined as the full width at half minimum of the attractive part of the potential, of the water/graphite potential for SPC/E and TIP4P are almost identical, both with $D=9.35$ kJ/mol and $w=0.135$ nm, if evaluated at $T=475$ K and using the water dipole moment of 1.85 D. Therefore we expect that T_w calculated from the CCST model using these two potentials will be comparable. If the simulation results in this work are taken to be standard, the predicted T_w of 474 K by the CCST model is very accurate indeed. It has been shown that the CCST model usually works well in predicting the wetting behavior involving spherical fluids such as inert gases, but it has not been tested extensively with nonspherical molecules. The fact that this simple model works well in predicting the wetting of water on graphite, although water has a very different kind of potential than inert gases, suggests that the model contains the essential physics of wetting.

The author is indebted to Peter T. Cummings and Milton W. Cole for many helpful discussions throughout this work. This research was conducted at the Center for Nanophase Materials Sciences, which is sponsored at Oak Ridge National Laboratory by the Division of Scientific User Facilities, U.S. Department of Energy.

*zhaox@ornl.gov

[1] J. W. Cahn, J. Chem. Phys. **66**, 3667 (1977).
[2] C. Ebner and W. F. Saam, Phys. Rev. Lett. **38**, 1486 (1977).
[3] G. Mistura, H. C. Lee, and M. H. W. Chan, J. Low Temp. Phys. **96**, 221 (1994).
[4] D. Ross, P. Taborek, and J. E. Rutledge, Phys. Rev. Lett. **74**, 4483 (1995).
[5] R. B. Hallock, J. Low Temp. Phys. **101**, 31 (1995).
[6] B. Demolder, N. Bigelow, P. Nacher, and J. Dupont-Roc, J. Low Temp. Phys. **98**, 91 (1995).
[7] A. F. G. Wyatt, J. Klier, and P. Stefanyi, Phys. Rev. Lett. **74**, 1151 (1995).
[8] M. Yao and F. Hensel, J. Phys.: Condens. Matter **8**, 9547 (1996).
[9] G. B. Hess, M. J. Sabatini, and M. H. W. Chan, Phys. Rev. Lett. **78**, 1739 (1997).
[10] D. Ross, J. A. Phillips, J. E. Rutledge, and P. Taborek, J. Low Temp. Phys. **106**, 81 (1997).
[11] V. F. Kozhevnikov, D. I. Arnold, S. P. Naurzakov, and M. E. Fisher, Phys. Rev. Lett. **78**, 1735 (1997).
[12] D. Ross, P. Taborek, and J. E. Rutledge, Phys. Rev. B **58**, R4274 (1998).
[13] F. Hensel and M. Yao, Ber. Bunsenges. Phys. Chem. **102**, 1798 (1998).
[14] Y. Ohmasa, Y. Kajihara, and M. Yao, J. Phys.: Condens. Matter **10**, 11589 (1998).
[15] Y. Ohmasa, Y. Kajihara, and M. Yao, Phys. Rev. E **63**, 051601 (2001).
[16] V. F. Kozhevnikov, D. I. Arnold, S. P. Naurzakov, and M. E. Fisher, Fluid Phase Equilib. **150**, 625 (1998).
[17] C. Ebner and W. F. Saam, Phys. Rev. B **35**, 1822 (1987).
[18] J. E. Finn and P. A. Monson, Phys. Rev. A **39**, 6402 (1989).
[19] E. Cheng, M. W. Cole, W. F. Saam, and J. Treiner, Phys. Rev. Lett. **67**, 1007 (1991).
[20] E. Cheng, M. W. Cole, W. F. Saam, and J. Treiner, Phys. Rev. B **48**, 18214 (1993).
[21] M. Wagner and D. M. Ceperley, J. Low Temp. Phys. **94**, 185 (1994).
[22] M. J. Bojan, M. W. Cole, J. K. Johnson, W. A. Steele, and Q. Wang, J. Low Temp. Phys. **110**, 653 (1998).
[23] M. Boninsegni and M. W. Cole, J. Low Temp. Phys. **110**, 685 (1998).
[24] F. Ancilotto and F. Toigo, Phys. Rev. B **60**, 9019 (1999).
[25] M. J. Bojan, G. Stan, S. Curtarolo, W. A. Steele, and M. W. Cole, Phys. Rev. E **59**, 864 (1999).
[26] S. Curtarolo, G. Stan, M. J. Bojan, M. W. Cole, and W. A. Steele, Phys. Rev. E **61**, 1670 (2000).
[27] F. Ancilotto, S. Curtarolo, F. Toigo, and M. W. Cole, Phys. Rev. Lett. **87**, 206103 (2001).
[28] W. Shi, J. K. Johnson, and M. W. Cole, Phys. Rev. B **68**, 125401 (2003).
[29] S. M. Gatica, J. K. Johnson, X. C. Zhao, and M. W. Cole, J. Phys. Chem. B **108**, 11704 (2004).
[30] J. R. Errington, Langmuir **20**, 3798 (2004).
[31] W. Shi, X. C. Zhao, and J. K. Johnson, Mol. Phys. **100**, 2139 (2002).
[32] H. J. C. Berendsen, J. R. Grigera, and T. P. Straatsma, J. Phys. Chem. **91**, 6269 (1987).
[33] B. Guillot, J. Mol. Liq. **101**, 219 (2002).
[34] D. Bonn and D. Ross, Rep. Prog. Phys. **64**, 1085 (2001).
[35] W. A. Steele, Surf. Sci. **36**, 317 (1973).
[36] X. C. Zhao and J. K. Johnson, Mol. Simul. **31**, 1 (2005).
[37] A. M. Ferrenberg and R. H. Swendsen, Phys. Rev. Lett. **61**, 2635 (1988).
[38] W. Shi and J. K. Johnson, Fluid Phase Equilib. **187**, 171 (2001).
[39] A. O. Parry and R. Evans, Phys. Rev. Lett. **64**, 439 (1990).
[40] I. C. Yeh and M. L. Berkowitz, J. Chem. Phys. **111**, 3155 (1999).
[41] P. Paricaud, M. Predota, A. A. Chialvo, and P. T. Cummings, J. Chem. Phys. **122**, 244511 (2005).